DALTON PERSPECTIVE

Tools of the trade in modeling inorganic reactions. From balls and sticks to HOMO's and LUMO's†

Tom Ziegler

University of Calgary, Dept. of Chemistry, 2500 University Drive NW, Calgary, T2N 1N4, Canada

Received 10th July 2001, Accepted 28th September 2001
First published as an Advance Article on the web 25th January 2002

The modeling of inorganic reactions requires access to accurate potential energy surfaces (PES) as well as theoretical methods that can deal with the dynamic movement on the PES of all atoms involved in the reaction. The first part of the overview assesses the accuracy by which various electronic structure theories can generate PES's for transition metal complexes. Considerations are also given to methods that deal with steric bulk and solvation effects as well as excited state PES's. The second part discusses the different dynamical and statistical methods available for the determination of reaction rates for a given PES.

1. Introduction

It has proven useful[1] to consider a chemical process as a sequence of one or more elementary reaction steps.

$$A + B \xrightarrow{k} C + D \qquad (1)$$

In each elementary step the chemical system moves from one minimum on the potential energy surface representing the reactants (A + B) over an energy maximum (the transition state) to another energy minimum characterized by the products (C + D), see Fig. 1, where the nature of the reactants and products as well as the magnitude of the rate constant k are established experimentally. Studies of elementary reaction steps in inorganic chemistry began in earnest after the Second World War with the experimental work of Basolo,[2] Pearson,[3] and others.[1]

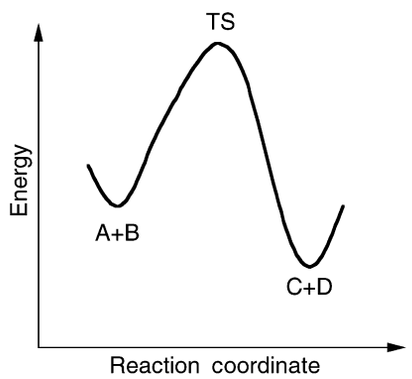

Fig. 1 Energy profile for the elementary reaction step A + B ⟶ C + D.

Quantum mechanics (QM) makes it in principle possible to determine the potential energy surface (PES) for a reacting system[4] such as the one given in eqn. (1) along with the structures of the species involved. Early attempts to make use of QM in the understanding of inorganic chemical reactions were based on rather approximate solutions to the fundamental underlying equations. They included the use of crystal-field theory (CF) to rationalize trends in the rate of ligand substitution reaction involving transition metal complexes,[1] as well as perturbational molecular orbital theory (PMO)[5] in which trends in rates are rationalized in terms of symmetry arguments[5] and the hardness[5c] and softness[5c] of the reactive centers on A and B.

Developments in both methodology and computer hardware have made it possible within the last decade to solve the fundamental QM equations with sufficient accuracy to obtain nearly quantitative information about the PES of a chemical system. This development will be reviewed in Section 2 where we also discuss how one can include the influence of the solvent and bulky substituents on the shape of the potential energy path (Fig. 1) of a chemical reaction for both the ground state and the higher lying excited states. It should be pointed out that the qualitative arguments based on PMO as they have been used in the past also would have a future place in rationalizing the results from modern quantitative calculations on chemical systems.

The energy profile in Fig. 1 conveys essentially only enthalpic information about the chemical reaction of eqn. (1) whereas the rate constant (k) and the equilibrium between A + B and C + D are related to the free energy of the system.[6] Thus, on top of the quantum mechanical calculations generating the PES we

† Based on the presentation given at Dalton Discussion No. 4, 10–13th January 2002, Kloster Banz, Germany.

Tom Ziegler was born in 1945 and raised in Denmark. He graduated from the University of Copenhagen in 1972 with a Cand. Scient. degree in theoretical chemistry. He obtained a Ph.D. from the University of Calgary (1978) where he has been a full Professor since 1991 and currently is holding a Canada Research Chair in theoretical inorganic chemistry. He has in the last 30 years worked on the development of density functional theory as a practical tool in transition metal chemistry and homogeneous catalysis. This has led to computational methods of use in spectroscopy, thermochemistry, structure determination and molecular dynamics. He is a fellow of both the Royal Danish and Royal Canadian Society.

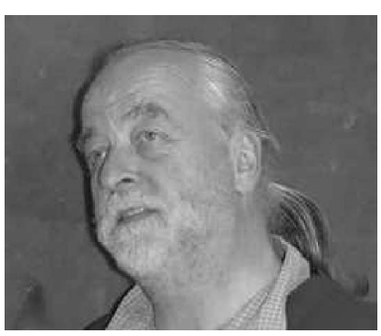

Tom Ziegler

 DOI: 10.1039/b106126g

need a statistical treatment that averages over different initial velocities of the atoms in A + B for the trajectories leading to the products C + D. The different ways in which this is done is the subject of Section 3.

Section 4 summarizes the state of the art of the computational methods used to model inorganic reaction mechanisms with a view towards new developments and novel applications.

2. Electronic structure theory and potential energy surfaces

The first part of the overview assesses the accuracy by which various electronic structure theories can generate PES's for transition metal complexes. Considerations are also given to methods that deal with steric bulk and solvation effects as well as excited state PES's

2.1. First principle determination of the potential energy surface

The many-electron Schrödinger equation

$$\hat{H}_T\Theta = E_T\Theta \tag{2}$$

can in principle provide a full description of a molecular system. In eqn. (2) the factor E_T is the energy of the system whereas Θ is a wavefunction that depends on the electronic and nuclear coordinates and $\hat{H}_T$ is the quantum mechanical Hamiltonian[4] of the molecule. It is customary to simplify eqn. (2) by considering the nuclei as fixed in space (the Born–Oppenheimer approximation[4]). In this case the Schrödinger equation is reduced to

$$\hat{H}\Psi = E\Psi \tag{3}$$

where Ψ is a function (the electronic wave function) that depends on the coordinates of the electrons whereas E is the potential energy $E(\vec{q}_1, \vec{q}_2, \vec{q}_3,..., \vec{q}_N)$ of the molecule at the nuclear coordinates $\{\vec{q}_i, i = 1, N\}$ and $\hat{H}$ is the Hamiltonian of the molecule with the kinetic energy of the nuclei omitted.[4] A complete knowledge of the potential energy surface $E(\vec{q}_1, \vec{q}_2, \vec{q}_3,..., \vec{q}_N)$ requires the solution of eqn. (3) at all nuclear conformations. Eqn. (3) can be solved to any degree of accuracy by expanding Ψ in terms of so-called Slater determinants[4] D_i as

$$\Psi = \sum_{i=1}^{m_o} f_i D_i \tag{4}$$

where

$$D_i = |\varphi_{i1}(1)\ \varphi_{i2}(2)\ \varphi_{i3}(3)\ \ldots\ldots\ldots\ \varphi_{in}(n)| \tag{5}$$

is a determinant with the general element for row k and column j given by the function $\phi_{ik}(j)$. Here (j) indicates the space and spin coordinates of electron j. The function $\phi_{ik}(j)$ is in turn expressed as a linear combination of a set of known functions $\{\chi_r; r = 1, m\}$ as

$$\varphi_{ik}(j) = \sum_{r=1}^{r=m} C_{ik,r}\chi_r(j) \tag{6}$$

Most often $\{\chi_r; r = 1, m\}$ is a set of atomic orbitals and the corresponding molecular orbitals $\phi_{ik}(j)$ are thus written as a linear combination of atomic orbitals (LCAO). The coefficients f_i and $C_{ik,r}$ of eqns. (4) and (6), respectively are determined in such a way as to minimize[4] the energy E of eqn. (3) which can also be written as

$$E = \int \Psi^* \hat{H} \Psi d\tau / \int \Psi^* \Psi d\tau \tag{7}$$

By increasing the number of determinant (m_o) as well as basis functions (m) exact solutions can be found for E and Ψ.

In the simple Hartree–Fock (HF) theory[4] only a single determinant D_o is used in the expansion for the wave function Ψ given in eqn. (4). HF calculations were first carried out on transition metal complexes around 1970,[7] often with very small basis sets. The time required to carry out HF calculations is formally proportional to m^4. However the use of an efficient algorithm reduces the time requirement to m^2. For large systems (> 1000 atoms) the time required scales linearly[8] with m. The HF method neglects correlation between the movements of electrons of different spins and has only been of limited success in terms of chemical accuracy for transition metal complexes. This is especially true for 3d metals.[9] However, the HF method can be applied routinely to large systems with up to 2000 atoms.

Correlation between electrons of different spins can be taken into account by including an increasing number of Slater determinants into the expansion for Ψ given in eqn. (4). Simpler correlated methods include the second order Møller–Plesset perturbation theory scheme[10] (MP2), the generalized valence bond method[11] (GVB) and the complete active space scheme[12] (CASSCF). These methods provide reasonable chemical accuracy with time requirements increasing as m^4 with the number of basis functions m. More accurate correlated methods include the coupled-cluster scheme CCSD(T), the multi-reference approach (MCSCF) as well as the complete active space second-order perturbation theory (CASPT2).[13] Especially CCSD(T) has been shown to provide high chemical accuracy.[9a] Unfortunately the CCSD(T) scheme requires large basis sets and scales as m.[6] Thus CCSD(T) can only serve as a bench-mark method for smaller size molecules (10 atoms). The correlation between electrons at close distance (dynamic correlation) is described well by the CCSD(T) scheme. However there are cases in which the correlation between electrons separated by long distances (non-dynamic correlation) is important as well. For these cases[9b] use must be made of MCSCF and CASPT2 approaches.

Kohn and Sham[14] have formulated an alternative way in which to obtain the potential energy E of eqn. (7) along with other molecular properties without solving for Ψ of eqn. (3). This method is often referred to as density functional theory (DFT).[15] It is based on a theorem of Kohn and Hohenberg[16] according to which the ground state energy E is determined uniquely by the electron density $\rho(\vec{r})$. Unfortunately, the exact relation between E and $\rho(\vec{r})$ is not known and the practicality of DFT has largely relied on finding approximate but accurate relations between E and $\rho(\vec{r})$ guided by physical arguments. Kohn[14] suggested as early as 1965 to write E as a function of $\rho(\vec{r})$ in what became known as the local density approximation (LDA). The LDA method affords reasonable geometries but tends to overestimate bond energies.[15d] Becke,[17] Perdew[18] and others[19] have, since 1980, formulated expressions for E in terms of $\rho(\vec{r})$ and its first derivative with respect to $\vec{r}$. These methods are collectively referred to as generalized gradient approximations[17b] (GGA) and considerably improves calculated bond energies compared to LDA.[9b,15a,d] Well-tested GGA methods are BP86,[17c,18a] BLYP,[19a] PBE,[18b] and RPBE.[19b,c] Most recently energy expressions containing $\rho(\vec{r})$ as well as its first derivatives and higher order terms have appeared. They are often referred to as Laplacian methods (LAP).[20] The LAP schemes are currently under evaluation for transition metal complexes. Another promising method is the self-interaction corrected DFT method (SIC-DFT).[20e,f]

For all the DFT methods[15] mentioned so far use is made of n (Kohn–Sham) orbitals to express the electron density of the n-electron system according to

$$\rho(\vec{r}) = \sum_{i=1}^{n} \varphi_i^*(\vec{r})\varphi_i(\vec{r}) \tag{8}$$

Table 1 Calculated and experimental M–C bond lengths (Å) for $M(CO)_6$ (M = Cr, Mo)[a]

Method	$Cr(CO)_6$ M–C	$Mo(CO)_6$ M–C
LDA	1.866	2.035
BP86	1.910	2.077
RPBE[a]	1.925	
B3LYP	1.921	2.068
HF	2.00	
MP2	1.883	2.066
CCSD(T)	1.939	
Exp.	1.918	2.063

[a] All data from ref. 15*a* except the RPBE results which were taken from ref. 23*b*.

where the KS-orbitals are expressed as a linear combination of basis functions

$$\varphi_i(\vec{r}) = \sum_{k=1}^{k=m} C_{ik}\chi_k(\vec{r}) \qquad (9)$$

For each DFT scheme the total energy is expressed in terms of the KS-orbitals and the expansion coefficients $\{C_{ik};\ i = 1, n;\ k = 1, m\}$ are determined in such a way as to minimize the energy. Thus the DFT approach requires only the optimization of the orbital coefficients C_{ik} whereas wave function methods in addition to the orbital coefficients also require the optimization of the determinant expansion coefficient $\{f_i;\ k = i, \text{large}\}$. This difference makes the DFT approach comparatively faster.

An interesting hybrid method suggested by Becke[21] mixes the Hartree–Fock energy expression with that from the the BLYP method. This scheme is referred to as B3LYP and is currently the most used approximate DFT method.

2.2. Accuracy of optimized molecular structures

Of great practical importance has been the development of methods that not only calculate potential energy points but also in an automated way locate local minimum energy points[22] representing stable structures. This is done by calculating the forces on all atoms (energy gradients) and stepwise moving the atoms in the direction of the forces towards lower energy until the nearest minimum is reached.[4] The ability to locate (optimize) molecular structures is likely the most important function of a modern electronic structure program.

Table 1 compares M–C bond distances calculated by different theoretical methods[15a,23b] to experiment for the series $M(CO)_6$ (M = Cr, Mo). We note among the DFT methods that LDA underestimates the M–C bond distances compared to experiment whereas the two GGA schemes BP86 and RPBE are in much closer agreement with experiment. It is in general observed that LDA M–L bonds are shorter than those obtained by the GGA schemes. Further, for covalent "organometallic bonds" (as in Table 1) the GGA schemes provide better bond distances than LDA. However, for ionic M–L bonds (L = halides[23c] or chalconides[23c,d]) the GGA bonds are too long and the LDA estimates are in some cases closer to the observed values.[23b] Tentative results seem to indicate that SIC-DFT considerably improves M–halide and M–chalconide bond distances.[20g] Also shown in Table 1 are M–C distances from the B3LYP hybrid method. They are seen to compare well with the GGA results. However, for distances between main group elements (as found in the ligand structures), the B3LYP performs somewhat better than the GGA schemes.[15a]

Let us next consider the wave function methods. Here for HF the Cr–C bond is seen to be much too long whereas it is too short for MP2. It is a general trend that MP2 over-corrects for the HF error in the case of 3d elements. For these elements CCSD(T) is often required in order to obtain accurate M–L distances. However, for the 4d element molybdenum (and its heavier congener, see later) MP2 is seen to be quite adequate, Table 1. The 3d elements are especially challenging because they have the *n*s, *n*p, and *n*d electrons ($n = 3$) in the same region of space. Thus ligand orbitals are strongly repelled by 3s, 3p as they are seeking stabilizing interactions with the 3d orbitals. The result is relatively long M–L distances and poor overlaps between the 3d set and the ligand orbitals. This in turn results in modest HUMO–LUMO gaps and a considerable amount of non-dynamic correlation.[23g] For the heavier congeners ($n = 4,5$) *n*s and *n*p are well separated from *n*d.

Table 2 First bond dissociation energies (FBDE's) for $Cr(CO)_6$ and $Mo(CO)_6$[a]

Method	FBDE/kcal mol^{-1} $Cr(CO)_6$	$Mo(CO)_6$
LDA	62.1	52.7
BP86	46.2	39.7
RPBE[a]	36.1	
B3LYP	40.7	40.1
HF	21.0	26.0
MP2	58.0	46.1
CCSD(T)	42.7	40.4
Exp.	36.8 ± 2	40.5 ± 2

[a] All data from ref. 9*a* except the RPBE results which were taken from ref. 23*b*.

2.3. Relative energies between reactants and products

Another test of the quality of the theoretical PES is the calculated relative energies between reactants and products. Table 2 displays the energies required to dissociate the first CO ligand from $M(CO)_6$ (M = Cr, Mo). We note among the DFT schemes that LDA overestimates the bond energy, and this is a general result for all M–L dissociations. For the GGA schemes, Table 2 and work by Rösch *et al.*[23a] seem to indicate that the RPBE is the most accurate method. However all the GGA schemes seem to afford M–L dissociation energies with an accuracy of ±5 kcal mol^{-1}. The data from Table 2 would indicate that B3LYP has an even smaller error margin. The performance of both BP86[9a,15a,24] and B3LYP[9a,15a,25] for transition metal complexes have been reviewed.

Among the wave function methods, the HF scheme finds the first CO dissociation energy to be too small for both metals with the larger error for chromium. The MP2 approach overcompensates for this by finding too strong an M–CO bond, especially in the case of chromium. Only CCSD(T) is able to afford a quantitative fit with experiment. It is in general found that M–L bond energies containing 3d elements require highly correlated methods (CCSD(T)) for a quantitative treatment. In many cases such a treatment is also recommended for 4d elements and their heavier congeners.[23f–h] It is possible to analyze the M–L bond strength in terms of donor/acceptor interactions and σ/π/δ bonding.[9c]

2.4. The importance of relativistic corrections for structures and energies

Valence electrons in atoms and molecules have a finite (albeit small) probability of being close to the nuclei and they can, as a consequence, acquire high instantaneous velocities. In fact, the velocities for valence electrons can approach that of light as they pass in close proximity to heavier nuclei with $Z > 72$. It is for this reason not too surprising that relativistic effects[26] become of importance for chemical properties of compounds containing 5d block elements in the third transition series.[27] The two main relativistic effects are the mass-velocity term, which takes into account that the mass of the electron is increased at high velocities, as well as the spin–orbit term. These effects can

Table 3 Calculated and experimental W–C bond distances (Å) and first W–CO bond dissociation energies (kcal mol^{-1}), FBDE's, for $W(CO)_6$ [a]

	$W(CO)_6$	
Method	W–C	FBDE
BP86 [b]	2.116	38.8
BP86 + R [c]	2.049	43.7
B3LYP [c]	2.078	44.8
HF		37.7
MP2 [c]	2.060	54.9
CCSD(T) [c]		48.0
Exp.	2.058	46.0 ± 2

[a] Data from ref. 9*c*. [b] Calculations without relativistic effects. [c] Calculations with relativistic effects included.

be included without considerably increasing the computational cost[27b] thanks to the development of a number of relativistic extensions to existing DFT and wave function methods.[27b]

Table 3 displays calculated and observed W–C bond distances and first W–CO dissociation energies. All entries, except BP86, are based on calculations with relativistic corrections included. We note that the non-relativistic BP86 calculations afford a W–C bond that is too long and too weak compared to experiment. By adding relativistic effects (BP86 + R) the bond is contracted by 0.067 Å and enhanced in strength by 4.9 kcal mol^{-1}. Both corrections considerably improve the agreement with experiment. The other relativistic calculations based on B3LYP and CCSD(T) afford estimates in similar good agreement with experiment. However HF and MP2 are again seen to respectively under-estimate and over-estimate the W–CO bond energy.

The relativistic bond contraction and stabilization for 5d elements are general phenomena. They are responsible for the experimental observation that M–L bonds for 4d elements often are slightly longer and somewhat more labile than the corresponding bonds involving a 5d element.[27b,28] This is shown in Fig. 2 for the M–O_2 bond dissociation energy[28] in $M(PH_3)_2$-

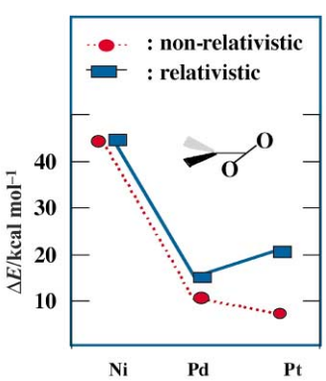

Fig. 2 Relativistic and non-relativistic M–O_2 bond energies for $(PH_3)_2M$–O_2 (M = Ni, Pd, Pt).

(μ-O_2) (M = Ni, Pd, Pt). The non-relativistic calculations provide a decrease in the M–O_2 bond energy. The introduction of relativity stabilizes the Pt–O_2 bond so that the oxygen bond to palladium is now the weakest. The origin of the relativistic bond contraction and stabilization can ultimately be traced back to the mass increase of valence electrons (mostly in s-orbitals) moving near the nuclei. This mass increase will reduce the kinetic energy, which in turn allows the bonds to contract, and stabilize.[26–29] The relativistic bond contraction and stabilization is especially important for compounds containing gold and mercury.[26,29a] However, it is also noticeable for actinides.[30]

2.5. Transition states and reaction paths

The transition state in Fig. 1 represents the lowest energy point on the ridge that separates the valley of the reactants from the valley of the products. It is characterized by having zero forces on all atoms as well as one and only one normal mode with an imaginary frequency. This normal mode defines the reaction coordinate of Fig. 1 in the vicinity of the transition state. The remaining part of the reaction coordinate in Fig. 1 is obtained by performing a steepest descent (in terms of energy) from the transition state to the reactants and the products, respectively. This pass is most often referred to as the minimum energy path (MEP) since its direction locally always is towards lowest energy. The reaction coordinate (RC) for the process is defined as all the conformations of the chemical system corresponding to points on the MEP, and the energy profile is the corresponding energy points on the PES.[31]

Locating transition states requires an element of chemical insight and has not yet been fully optimized from the specification of the reactants and the products. Strategies involve: (a) finding the ridge separating reactants and products, and searching for the minimum point on the ridge,[32a] (b) converging an initial path from reactants to products towards the MEP by iteratively finding new paths in which forces perpendicular to the reaction coordinate are minimized;[32b] (c) searching along a preconceived reaction coordinate,[32c] (d) following a normal mode with an imaginary frequency towards higher energies.[32d,e] Ultimately, the determined structure must have zero forces on all atoms and only one imaginary frequency to qualify as a transition state. Further the corresponding reactants and products can be found by a steepest descent to the nearest minimum.

Constructing the MEP can be a useful tool in a more detailed study of a chemical reaction. To this end consider the O–H activation of methanol by $CrCl_2O_2$ to produce $CrCl_2(O)(OH)$-(OCH_3), Scheme 1. The process has a four center transition state (TS1 of Scheme 1). Fig. 3 displays the change in the internal

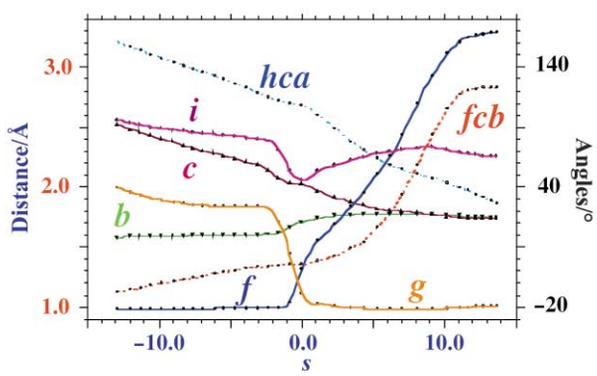

Fig. 3 Change in internal coordinates along the MEP for the reaction $CrCl_2O_2 \longrightarrow CrCl_2(O)(OH)(OCH_3)$. Reactants ($s = -10$); transition state ($s = 0.0$) and products ($s = 10.0$).

coordinates of the reaction system from reactants ($s = -10$) over the transition state ($s = 0.0$) to the products ($s = 10.0$), where s is the length of the MEP from the transition state (counted negative in the direction of the reactant). We note that the OH methanol bond (f of TS1 in Scheme 1) is broken just before the transition state whereas the new OH bond (g of TS1 in Scheme 1) is formed right after the transition state. Note also a decrease in the Cr–H bond at $s = 0$, as the metal assists the passage of hydrogen from one oxygen to another.

2.6. Representing steric bulk

The computational modeling of inorganic reactions necessitates, as we have seen, a high level quantum mechanical treatment because lower level methods cannot accurately treat the bond breaking and forming that occurs during these

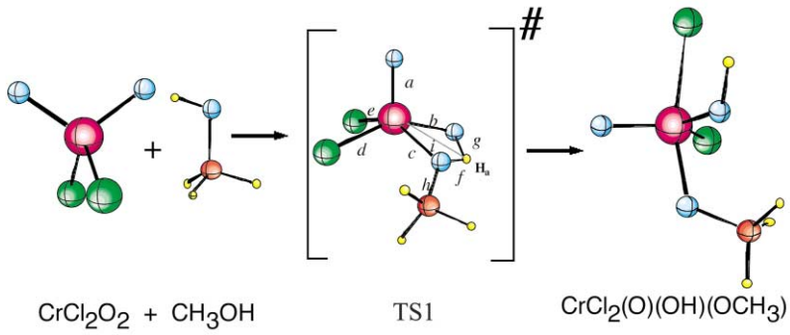

Scheme 1 Schematic presentation of the structural changes in the reaction $CrCl_2O_2 \longrightarrow CrCl_2(O)(OH)(OCH_3)$.

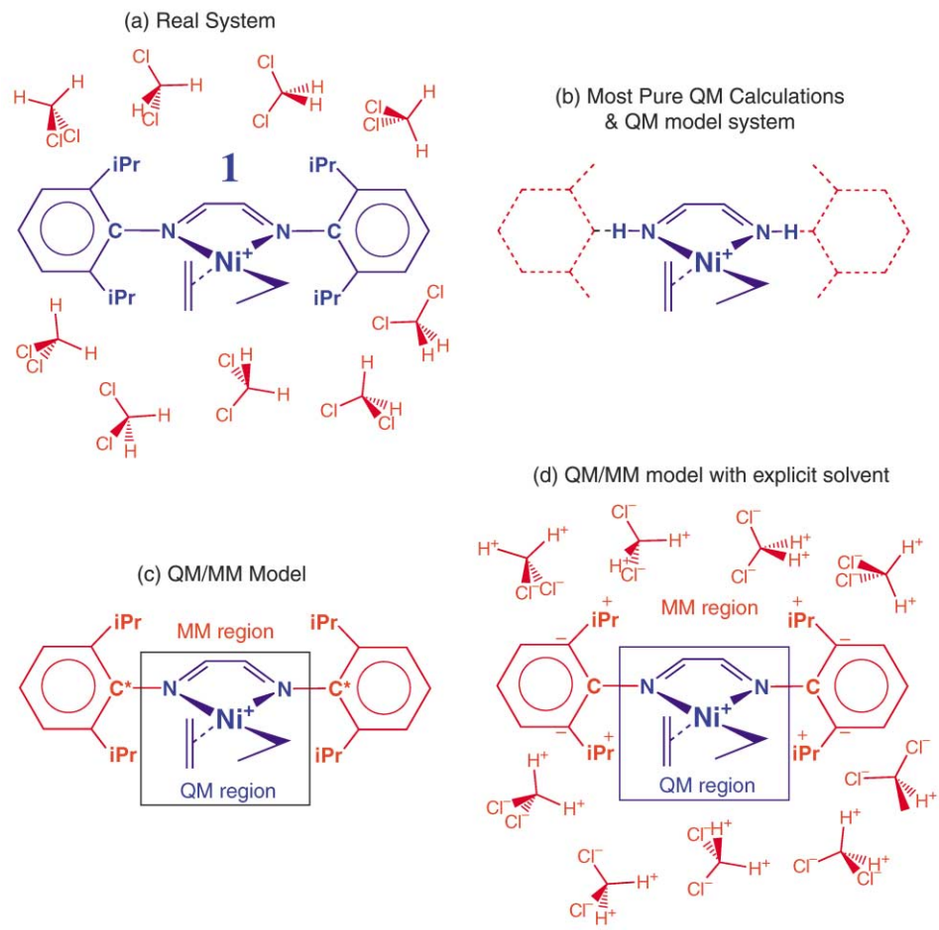

Fig. 4 The Brookhart Ni(II) bisimine catalyst.

processes. However, a high-level quantum mechanical study often involves a stripped down model system that only vaguely resembles the true system. An example of this is depicted in Fig. 4 where the 'real' catalyst system that is being modeled is shown in (a), while a likely model of it used for a quantum mechanical calculation is shown in (b). Thus, if large ligands are involved, they are most often neglected in high level calculations with the hope that they do not substantially influence the nature of the reaction mechanisms. Unfortunately, the surrounding ligand system, protein matrix, or solvent can often play a critical mechanistic role. One dramatic example in organometallic catalysis is that of the recently developed Ni(II) Brookhart polymerization catalyst,[34] **1** (Fig. 4). Without an extended ligand system the catalyst acts only as a dimerization catalyst. However, by attaching an extended and sterically demanding ligand system, Brookhart and co-workers were able to transform the poor polymerization catalyst into a commercially viable one. Therefore, quantum mechanical models which do not treat the extended ligand structure or solvent environment may yield results which are inconclusive, suspect or possibly erroneous. Even with the rapid development of computer technology and modern linear scaling methods (Section 2.1),[8,35] the full quantum mechanical treatment of these extended systems is not expected to be practical in the near future.

One reasonable approach to escape this problem is the combined quantum mechanics and molecular mechanics (QM/MM) method.[36] In this hybrid method part of the molecular PES, such as the active site region, is determined by a quantum mechanical calculation while the remainder of the molecular potential is determined using a much faster molecular mechanics force field calculation. Such a partitioning is illustrated in Fig. 4c. The promise of the QM/MM method is that it allows for simulations of bond breakage and formation at the active site, while still allowing for the role of the extended system to be modeled in an efficient and computationally tractable manner. The key feature of the QM/MM method is that the QM calculation is performed on a truncated "QM model" (Fig. 4b) of the active site, where the large ligands have been removed and replaced with capping atoms (in the current case hydrogens).

Then, a molecular mechanics calculation is performed on the remainder of the system and the effects of the attached ligands are incorporated to form the potential surface of the whole system where the QM and MM regions interact with one another *via* steric and electrostatic potentials.

The combined QM/MM methodology dates back to work by Warshel and Levitt[36a] in 1976, but it was not until 1986 that a practical QM/MM prescription was developed by Singh and Kollman.[36b] Despite its history, QM/MM methods have only recently received serious attention as a practical modeling tool to examine extended systems too large for pure QM methods. The QM/MM modeling of proteins has also been successful despite the impressive challenges that these complicated macromolecules impose. An area which has only begun to be explored with hybrid QM/MM potentials is transition metal containing catalytic systems, such as metalloenzymes[37a] and organometallic complexes.[37b] It is also possible to make hybrids between different levels of purely quantum mechanical methods.[37c] In all cases care must be given to how one divides up the chemical system as well as to how one stitches the different regions together afterwards.[37d] It is worth mentioning that a pure molecular mechanics (MM) approach has been used successfully in many cases, especially those not involving bond breaking or bond formation.[37e] We shall now in the next section discuss how one can incorporate the influence of the solvents shown in Fig. 4d.

2.7. Solvation effects

The presence or absence of solvent in a chemical system can lead to completely different chemical behaviour and reactivity. For this reason, the incorporation of solvent effects into quantum mechanical potential energy surfaces has been and still is an active area of theoretical chemistry. Methods for introducing solvent effects in quantum chemical calculations can be broadly divided into two categories[38] (i) continuum models[39–41] and (ii) explicit solvent models. With continuum models the solvent molecules are not treated explicitly but rather they are expressed as a homogeneous medium characterized by a bulk dielectric constant. This is shown pictorially in Fig. 5a. The effect of the solvent is modeled by a buildup of

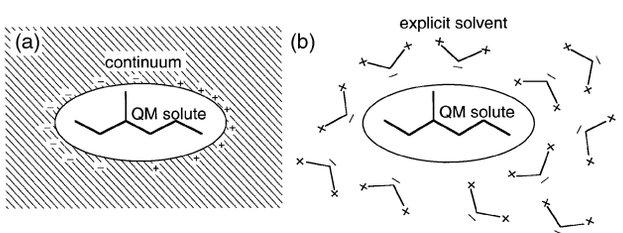

Fig. 5 Modeling solvation with (a) a continuum model and (b) explicit solvent molecules.

charge[42] on the continuum surface such that there is a polarization of the QM wave function within the solute cavity. The amount of charge buildup and subsequently the polarization of the wave function is a function of the dielectric constant of the solvent. Continuum models have been quite successful in capturing the general aspects of solvation and in many cases can be used for quantitative predictions. Since the solvent molecules are not treated explicitly, continuum models are relatively efficient. On the other hand, the lack of an explicit treatment has the disadvantage that continuum models do not provide any specific information concerning the intermolecular interactions.[43] The two most popular continuum methods are the polarizable continuum method (PCM),[40] and the conductor-like screening model (COSMO).[39]

The other broad approach to introducing solvent effects into the quantum mechanical potential surface is to treat the solvent molecules explicitly. With standard electronic structure calculations, this is achieved by surrounding the solute molecule with solvent molecules—all of which are treated quantum mechanically. For *ab initio* level calculations, generally only a few solvent molecules can be included. Although the interactions between the solvent molecules and solute molecule are treated rigorously—a few solvent molecules does not simulate the bulk solvent. Therefore, even qualitative conclusions can be dubious in nature. Recently, the Car–Parrinello[44] molecular dynamics method (see later) has allowed for simulations of bulk liquid to be carried out at the density functional level.[45,46] Although the approach is promising, it is still impractical for anything but the smallest solute and solvent molecules (*e.g.* water in water and methanol in water). The combined quantum mechanics and molecular mechanics (QM/MM) approach seems well suited for performing explicit solvation simulations. A natural partition exists such that the solute is treated with quantum mechanics, while the explicit solvent molecules are handled by a much more efficient MM force field. Pioneering the approach, Gao and co-workers,[47] have demonstrated that the QM/MM method can be used to predict solvent polarization effects at the quantitative level for such properties as reaction barriers, equilibrium constants and solvation free energies. Explicit solvation will be under development as an active research area for the next 10 years.[48] Meanwhile continuum models are likely to be used extensively in the day-to-day modeling of chemical reactions.

Table 4 Experimental and theoretical dipole-allowed excitation energies in $Ni(CO)_4$[a]

Method	Band-I	Band-II	Band-III	Band-IV
CASSCF	7.3	7.5	7.6	7.7
CASPT2	4.3	5.2	5.6	6.3
SAC-CI	4.8	5.5	5.7	5.8
TDDFT	4.7	4.8	5.4	5.8
Exp.	4.5	5.4	5.5	6.0

[a] All data (in eV) from ref. 49.

2.8. Excited states

We have up to now only discussed the PES for the ground state. However, at higher energies are the potential energy surfaces of the excited states. These surfaces have been probed experimentally by spectroscopic and photochemical methods.[47] For transition metal complexes crystal- and ligand-field theory has been used extensively to rationalize the large body of experimental data.

The first *ab initio* wave function calculations[7a] on transition metal excitation energies met with very little success as they included no HF or limited electron correlation. This is perhaps not so surprising since the degree of electron correlation can differ between two excited states or between the ground state and an excited state. It is now clear that highly correlated methods are required for a proper description of excited states. This is underlined in Table 4 where experimental[50] excitation energies for $Ni(CO)_4$ are compared to those obtained by CASSCF,[12] CASSPT2[13] and the symmetry-adapted cluster configuration interaction (SAC-CI)[51] scheme. It is noteworthy that the CASSCF method, with a fair degree of correlation, fails to represent the absolute value of the excitation energies as well as the spacing between them. However the very expensive CASSPT2 and SAC-CI schemes both reproduce the observed spectrum well.

DFT is in its original formulation a ground state theory.[16] However, it has been common practice to apply it to excited states by promoting electrons to KS-orbitals (eqn. (8)) of higher energy[52] than those occupied in the ground state. This procedure has been termed DFT-ΔSCF and it has been used extensively. In fact, the first DFT calculations in chemistry

Table 5 Experimental and theoretical dipole-allowed excitation energies in MnO_4^- [a]

Method	Band-I	Band-II	Band-III	Band-IV
SAC-CI	2.57	3.58	3.72	5.82
DFT-ΔSCF	2.57	3.42	3.76	5.99
TDDFT	2.63	3.60	4.52	5.46
Exp.	2.27	3.47	3.99	5.45

[a] All data (in eV) from ref. 49.

successfully made use of schemes[53] similar to DFT-ΔSCF in calculations on excitation energies for transition metal complexes. Quite recently a rigorous theory has been developed for the calculation of excitation energies within the framework of DFT.[54] The theory is based on time-dependent perturbation theory (TDDFT),[54d] and it has even been extended to the optimization of excited state structures.[54e] Table 4 illustrates that the excitation energies calculated by TDDFT for $Ni(CO)_4$ are of the same quality as those obtained by the much more expensive CASSPT2 and SAC-CI wave function methods

The electronic spectrum of the permanganate ion MnO_4^- has served[50,55] as a testing ground for new computational methods, and only few have passed the test due to the complicated electronic structure[23g] of this seemingly simple system. It is clear[50] from Table 5 that DFT-ΔSCF, TDDFT and SAC-CI all reproduce the electronic spectra with reasonable accuracy, although the assignment of the second and third band differ among the methods (not shown).[50] Unfortunately, the CASSPT2 scheme is too expensive for this molecule.[50]

It is likely that TDDFT (and to some degree DFT-ΔSCF) increasingly will be used to explore the excited state potential energy surfaces of inorganic molecules, and many applications on large molecules[56] have already appeared. In this respect the less expensive DFT-ΔSCF scheme can be used to map out the variation of the energy with geometry whereas TDDFT can provide more accurate energy information at particular geometries. The role of the more expensive CASSPT2 and SAC-CI wave function methods will be to serve as benchmark methods for smaller molecules.

3. The determination of reaction rates from the potential energy surface

Reaction rates are macroscopic averages over a large number of "chemically identical systems" passing with different initial velocities from the reactant valley to the product valley. Thus in order to determine the rates one must either perform a large number of trajectories in a dynamic approach or introduce statistical theories based on ensemble distributions.

3.1. Dynamical approaches

More than one decade ago theoretical chemists concerned with electronic structure theory and the calculation of PES had little interaction with theoreticians exploring reaction dynamics. In fact, dynamic studies were more often based on empirical PES's. This situation is rapidly changing as electronic structure theory has matured and now is able to provide accurate PES's.

3.1.1. Classical trajectories with empirical or first principle PES's. In classical trajectory calculations the nuclei are allowed to move on the potential surface according to Newton's classical laws of motion (eqn. (10))

$$m_i \frac{\partial^2 \vec{x}_i}{\partial t^2} = -\frac{\partial E(\vec{x}_1, \vec{x}_2, \ldots, \vec{x}_i, \ldots \vec{x}_N)}{\partial \vec{x}_i} \quad i = 1, 2 \ldots N_{\text{nuc}} \quad (10)$$

Thus, the position $\vec{x}_i(t + \Delta t)$ of particle i at time $t + \Delta t$ can be deduced from the position, velocity and force at t as

$$\vec{x}_i(t + \Delta t) = \vec{x}_i(t) + \frac{\delta \vec{x}_i(t)}{\delta t}\Delta t - \frac{1}{2m_i}\frac{\delta E}{\delta \vec{x}_i}\Delta t^2 \quad (11)$$

This method has not been used much for inorganic systems where empirical PES's are unreliable in the transition state region of reactions involving bond making and bond breaking. Use could have been made of PES's from electronic structure calculations. However, fitting multi-dimensional functions with more than two nuclei is a formidable and in practice intractable task.

Alternatively, the energy gradient $-\mathrm{d}E/\mathrm{d}x$ (eqn. (10)) needed to determine the position at $\vec{x}_i(t + \Delta t)$ (eqn. (11)) can be calculated directly by *ab initio* methods. This procedure has been termed direct dynamics.[57] It requires a full electronic structure calculation in which the expansion coefficients of eqn. (9) $\{C_{ik}; i = 1, n; k = 1, m\}$ are fully optimized *for each time step*, Δt. Since some 10000 time steps are required in one trajectory, this method is still too expensive for all but the smallest of systems. The propagation of the atoms on a potential surface according to eqns. (10) and (11) is often referred to as molecular dynamics (MD).

3.1.2. Car–Parrinello molecular dynamics. In 1985 Car and Parrinello[58] developed a direct dynamics scheme in which the orbital coefficient $\{C_{ik}; i = 1, n; k = 1, m\}$ formally are considered as dynamic quantities with fictitious masses μ and propagated in time according to

$$\mu \ddot{c}_{i,k} = -\frac{\partial E}{\partial c_{i,k}} - \sum_j \lambda_{i,j} c_{i,k} \quad (12)$$

parallel to the nuclear positions according to eqn. (10).

Formally, the nuclear and electronic degrees of freedom are cast into a single, combined Lagrangian:

$$L = \frac{1}{2}\sum_{i=1}^{n} \mu_i \left\langle \frac{\delta \varphi_i}{\delta t} \middle| \frac{\delta \varphi_i}{\delta t} \right\rangle + \frac{1}{2}\sum_{i=1}^{I=N} m_I \frac{\delta \vec{x}_I}{\delta t} \bullet \frac{\delta \vec{x}_I}{\delta t} - E(\varphi_i\rangle, \vec{x}_I) + \sum_{i,j} \Lambda_{ij} \langle \varphi_i \varphi_j \rangle \quad (13)$$

where the first two terms represent the kinetic energy of the wave function and nuclei, respectively, the third term is the potential energy and the last term accounts for the orthogonality constraint of the orbitals. If the fictitious masses are such that the fictitious kinetic energy of the wave function is very small compared to the physically relevant kinetic energy of the nuclei, then the Car–Parrinello method propagates the electronic configuration very near to the proper Born–Oppenheimer surface. The generated electronic structure oscillates around the Born–Oppenheimer surface, which over time gives rise to stable molecular dynamics. The coupled Car–Parrinello dynamics, therefore, result in a speed up over conventional direct dynamics since the electronic wave function does not have to be converged at every time step, instead it only has to be propagated. The primary disadvantage of the Car–Parrinello scheme is that the electronic configuration oscillates about the Born–Oppenheimer wave function at a high frequency. Therefore, in order to generate stable molecular dynamics a very small time step must be used, usually an order of magnitude smaller than in conventional *ab initio* molecular dynamics. The CP method has been used to study the trajectory from the transition state to the products and reactants in a number of organometallic reactions.[59] Such studies are highly informative but do not provide quantitative information about reaction rates due to the limited number of studied trajectories. The CP method has been extended to include QM/MM[60a] and the COSMO[60b] solvation model. The CP method is an example of an *ab initio* molecular dynamics method (AIMD) since no empirical input is needed.

3.1.3. Quantum dynamics with fitted or empirical PES's. Quantum dynamics makes use of the time-dependent Schrödinger equation for a system

$$-\frac{\hbar}{i}\frac{\partial \Psi}{\partial t} = -\sum_{i=1}^{i=N}\frac{\hbar^2}{2m_i}\nabla^2\Psi + E\Psi \qquad (14)$$

of N nuclei with the potential energy E. The method is only feasible for up to three nuclei. However, for larger molecules the remaining degrees of freedom can be treated as 'background'. Quantum dynamics has been used extensively for hydrogen containing systems where tunneling might be of importance. Examples from inorganic chemistry are absorption of H_2 on metal surfaces,[61a] exchange of hydrogen between hydride and di-hydrogen ligands[61b] in transition metal complexes, photo-dissociation of H_2[61c] or H[61d] from metal complexes. It is likely that this method will be used extensively to probe quantum effects in processes involving hydrogen atom transfer[61e] where quantum effects such as tunneling will be especially important.

3.2. Statistical approaches

The most well known statistical approach to the calculation of reaction rates is the transition state theory by Eyring in which the degrees of freedom perpendicular to the reaction coordinate at the transition state are assumed to be in thermal equilibrium with degrees of freedom of reactants and products. The rate constant for reactions in the condensed phase can, according to the transition state theory by Eyring, be written as

$$k = \kappa\frac{k_B T}{h}\exp[-\Delta G^{\#,0}(T)/RT] \qquad (15)$$

where $\Delta G^{\#,0}$ is the standard-state free energy of activation, k_B is the Boltzmann constant, h Plank's constant and κ the transmission constant. The κ factor takes into account the probability of trajectory recrossing over the transition state ridge as well as non-equilibrium and quantum effects. However, it is often taken as $\kappa = 1$. We shall in the following discuss how the transition state theory is used in practical calculations.

3.2.1. Transition state theory based on the harmonic approximation. In conventional transition state theory $\Delta G^{\#,0}$ is evaluated[62a] at the saddle point of the PES of the reaction (Fig. 1) using standard expressions from statistical mechanics[62] based on the relative energies, vibrational frequencies, total masses and moments of inertia of reactants, transition states, and products. The vibrational frequencies are readily available from electronic structure calculations within the harmonic approximation.[62a] In the variational transition state theory (VTST) by Truhlar and Garrett[62b] $\Delta G^{\#,0}$ is taken at the top of a minimum *free* energy path (MFEP) that connects reactants and products rather than at the top of the MEP. However, the extra cost has so far prevented the application of VTST to transition metal complexes.

A systematic study on the performance of different theoretical methods with respect to the calculation of activation barriers and free energy of activation is available for organic reactions[63] but not yet for inorganic processes. The most extensive evaluations are on coordinatively unsaturated metal ions attached to a single organic molecule[64a,b] or ligand.[64c] However, these seemingly simple systems have an electronic structure that is much more complex than larger coordinatively saturated complexes. Some comparisons between theory and experiment have been carried out for ligand substitution processes in octahedral[65] and square planar complexes,[66] migratory insertion of CO[61b] and ethylene[67] into metal–alkyl bonds, and oxidative addition of H–H[68a] and H–C[68b] bonds to metal centers. The picture emerging from the limited data is similar to that reached for thermodynamic properties.[9c] Thus among the wave function methods CCSD(T) is required for 3d elements to obtain accurate barriers (± 5 kcal mol^{-1}) whereas the lower level MP2 theory can be used in some cases for 4d and 5d elements. For DFT the GGA schemes (PB86 and RPBE) as well as B3LYP afford in most cases kinetic barriers within 5 kcal mol^{-1}.

A number of excellent review papers have already appeared on the application of first principle methods to inorganic reactions based on the Eyring transition state theory. They cover studies on ligand substitution reactions,[69] insertion reactions,[69,70a] oxidative addition,[69,70b,e] nucleophilic[69a] and electrophilic[69a] attack as well as metallacycle formation[70c,d] and surface chemistry.[71] Reviews are also available on application to homogeneous[72a] and heterogeneous[72b,c] catalysis as well as metalloenzymes.[72d-f]

3.2.2. Transition state theory based on thermodynamic integration. The harmonic approximation used above is excellent in many cases. However, for processes where weak intermolecular forces dominate, the harmonic or quasi-harmonic approximation breaks down.[73] In these cases *ab initio* molecular dynamics simulations (Section 3.1.2) can be utilized to determine reaction free energy barriers. An MD simulation samples the available configuration space of the system to produce a Boltzmann ensemble from which a partition function can be constructed and used to determine the free energy. However, finite MD simulations can only sample a restricted part of the total configuration space, namely the low energy region. Since estimates of the absolute free energy of a system requires a global sampling of the configuration space, only relative free energies can be calculated.

A number of special methodologies have been developed to calculate relative free energies. Since we are interested in reaction free energy barriers, the method of choice is derived from the method of thermodynamic integration.[74] Assuming we are sampling a canonical NVT ensemble the Helmholtz free energy difference, ΔA, between an initial state with $\lambda = 0$ and a final state with $\lambda = 1$, is given by eqn. (16).

$$\Delta A(0 \rightarrow 1) = \int_0^1 \frac{\partial A(\lambda)}{\partial \lambda}\mathrm{d}\lambda \qquad (16)$$

Here the continuous parameter λ is such that the potential $E(\lambda)$ passes smoothly from initial to final states as λ is varied from 0 to 1. Since the free energy function can be expanded in terms of the partition function:

$$A(\lambda) = -kT\ln\left[\int\ldots\int \mathrm{e}^{\frac{E(X^N,\lambda)}{kT}}\mathrm{d}X^N\right] \qquad (17)$$

the relative free energy ΔA can be rewritten as:

$$\Delta A(0 \rightarrow 1) = \int_0^1\left(\int\ldots\int\frac{\partial E(X^N,\lambda)}{\partial\lambda}\mathrm{d}X^N\Big|_\lambda\right) \qquad (18)$$

or

$$\Delta A(0 \rightarrow 1) = \int_0^1\left\langle\frac{\partial E(X^N,\lambda)}{\partial\lambda}\right\rangle_\lambda \mathrm{d}\lambda \qquad (19)$$

where the subscript λ represents an ensemble average at fixed λ. Since the free energy is a state function λ can represent any pathway, even non-physical pathways. However, the ideal choice is the MEP. The reaction coordinate can be sampled with discrete values of λ on the interval from 0 to 1 or carried out in a continuous manner in what is termed a "slow growth" simulation[74a] by

$$\Delta A = \sum_{i=1}^{N_{steps}}\left\langle\frac{\partial E(\lambda)}{\partial\lambda}\right\rangle_i \Delta\lambda_i \qquad (20)$$

where *i* indexes the step number. Here the free energy difference becomes the integrated force on the reaction coordinate and can be thought of as the work necessary to change the system from the initial to the final state. The discrete sampling resembles a linear transit calculation such that a series of simulations is set up corresponding to successive values of the reaction coordinate from the initial to the final state. For each sample point, the dynamics must be run long enough to achieve an adequate ensemble average force on the fixed reaction coordinate. In a slow growth simulation[74a] the reaction coordinate is continuously varied throughout the dynamics from the initial to the final state. Thus, in each time step the reaction coordinate is incrementally changed from that in the previous time step.

Margl and co-workers have pioneered the use of the slow growth method in studies of reactions involving metal complexes with AIMD. These studies include C–H activation[75a] of methane by a Rh(I) complex, CO insertions into metal–alkyl bonds,[60b,75b] olefin insertion into the metal–ethyl bond of $[Cp_2Zr(C_2H_5)]^+$[75c] and $[(CpSiH_2NH)Ti(C_2H_5)]^+$,[75d] chain termination in $[(CpSiH_2NH)Ti(C_2H_5)]^+$,[75e] formation of a dihydrogen allyl complex from $[(CpSiH_2NH)Ti(C_2H_5)]^+$,[75f] olefin complexation to Ni(II).[75g] The application of the slow growth method to transition metal complexes has been reviewed.[75h–j] The slow growth method has been extended to include QM/MM[60a] and the COSMO[60b] solvation model. Both discrete sampling[76a] and slow growth[76b] is ideally suited to simulate explicit solvation.

4. Concluding remarks about potential energy surfaces and dynamics

Electronic structure theory has, over the past 10 years, progressed to the point where it is possible to describe the potential energy surface of a gas phase molecule containing up to 10 atoms with great accuracy using high level wave function methods such as CCSD(T) (ground state) or CASSPT2/SAC-CI (excited states). For larger systems acceptable accuracy can be obtained by DFT (ground state) or TD-DFT/ΔSCF-DFT (excited states). Great strides have also been taken in describing the PES for reactions on surfaces[71a] at the interface between gas phase and solid state. Here DFT will continue to be the electronic structure theory of choice.[19b] Of special importance for transition metals is the development of methods that include relativistic effects since they are required to describe periodic trends correctly within a triad of transition metals. As hardware becomes faster larger molecules can be treated with higher accuracy using existing methodology. Known methods are also likely to become faster by neglecting interactions between fragments in large molecules that are 'far apart'. In this way most methods will eventually become linear[8] in the number of atoms if this number is large enough. It is finally possible that further progress in approximate DFT will result in new methods with the same accuracy as highly correlated wave functions and speeds still comparable to GGA-DFT.

Many chemical systems of interest have large bulky groups that exert steric pressure on the reactive center (Fig. 4) as an essential part of how they function. For such systems increasing use will be made of dual- or multi-level approaches in which the steric bulk is treated at a lower level of theory than the reactive system.[36,37] The reason that one would like to treat bulky groups by MM is not only that they have a large number of electrons but also (rather) that they potentially possess a formidable number of conformations. The many conformations make it difficult (expensive) to determine the global energy minimum even with MM.

Solvent effects can have a profound impact on chemical reactions, yet we do not at the moment have a proven methodology (as in the case of electronic structure theory) that by well known routes can converge to chemical accuracy. Continuum methods[39,41] are going to carry the bulk of the workload in the foreseeable future. However, it will be one of the major challenges within the next decade to develop solvation theories that by standard procedures will converge to chemical accuracy. Such methods are likely to combine explicit solvation for the first few solvation shelves with bulk descriptions (continuum or mean-field)[77] for the remaining part of the solvent.[43,47]

Turning next to dynamics on the PES and calculations of reaction rates, one might expect that these rates for the majority of cases will be determined with the help of Eyring's transition state method. To this end, locating saddle points on the PES is still time consuming in terms of manpower, and more systematic and automated procedures would be welcome.[32]

The standard applications of Eyring's transition state method make use of a saddle point along the MEP (the transition state) as well as frequencies based on the harmonic approximation. Thus, standard applications will not be possible for reactions without an enthalpic barrier (most radical recombination processes and acid–base reactions)[75g] or for reactions with many low frequency modes (such as processes in solution with several explicit solvent molecules included, nucleation and folding of large molecules). In those cases the free energy of activation will have to be determined from methods based on thermodynamic integration[74] and the variational transition state method.[62b] Finally for reactions involving light atoms factors such as hydrogen tunneling effects will have to be taken into account.[61]

For the dynamical motion on excited state surfaces one has to deal with adiabatic crossings from one potential energy surface to another in problems related to photochemistry and electron transfer. This area is still under development with new promising theories[78a] and implementations/applications.[78b] The status of dynamic calculations on PES's has recently been reviewed.[78c]

The number of studies of inorganic reaction mechanisms by theoretical methods has increased drastically in the last decade. The studies cover ligand substitution reactions,[69] insertion reactions,[69,70a] oxidative addition,[69,70b,e] nucleophilic[69a] and electrophilic[69a] attack as well as metallacycle formation[70c,d] and surface chemistry,[71] in addition to homogeneous[72a] and heterogeneous[72b,c] catalysis as well as metalloenzymes.[72d–f] We can expect the modeling to increase further both in volume and sophistication.

It is still not clear how large a role modeling will play in practical applications such as catalyst design. It is true that modeling can provide insight as an alternative to the experimental approach of trial and error. However with the introduction of combinatorial chemistry the "trial and error" approach has been automated and accelerated to the point that it is highly competitive with designs based on fundamental insight. Perhaps this challenge will have to be met with the development of combinatorial computational approaches.

Acknowledgements

I would like to thank the present or former students: L. Fan, L. Versluis, T. K. Woo, K. Vanka, J. Cooper, I. Hristov, L. Deng and E. Zurek as well as former or present post-doctoral fellows: A. Michalak, P. Margl, R. Schmid, H. M. Senn, S. Tobisch, T. Firman, and D. Deubel. This work was supported by the Natural Sciences and Engineering Research Council (NSERC) as well as the donors of the Petroleum Research Funds, administered by the American Chemical Society (ACS-PRF No. 36543-AC3).

References

1 (*a*) R. B. Jordan, *Reaction Mechanisms of Inorganic and Organometallic Systems*, Oxford University Press, Oxford, 1991; (*b*) J. D. Atwood, *Inorganic and Organometallic Reaction Mechanisms*, VCH, 1997.

2 D. F. Shriver, *Coord. Chem. Rev.*, 1990, **99**, 3.
3 P. C. Ford, *Coord. Chem. Rev.*, 1999, **187**, 3.
4 I. R. Levine, *Quantum Chemistry*, Prentice Hall, New Jersey, 5th edn., 2000.
5 (*a*) M. J. S. Dewar, *Adv. Chem. Phys.*, 1965, **8**, 65; (*b*) R. B. Woodward and R. Hoffmann, *The Conservation of Orbital Symmetry*, Verlag Chemie, Berlin, 1970; (*c*) R. G. Pearson, *Symmetry Rules for Chemical Reactions*, John Wiley and Sons, New York, 1976; (*d*) T. A. Albright, J. K. Burdett and M.-H. Whangbo, *Orbital Interactions in Chemistry*, John Wiley & Sons, New York, 1985; (*e*) K. Fukui, *Acc. Chem. Res.*, 1971, **4**, 57.
6 S. Glasstone, K. J. Laidler and H. Eyring, *The Theory of Rate Processes*, McGraw-Hill, New York, 1941.
7 (*a*) I. H. Hilliers and V. R. Saunders, *Chem. Commun.*, 1969, 1275; (*b*) J. Demuynck and A. Veillard, *Chem. Phys. Lett.*, 1970, **6**, 204.
8 C. Ochsenfeld, C. A. White and M. Head-Gordon, *J. Chem. Phys.*, 1998, **109**, 1663.
9 (*a*) M. Diedenhofen, T. M. Wagener and G. Frenking, in *Computational Organometallic Chemistry*, ed. T. R. Cundari, Marcel Dekker, Basel, 2001, p. 69; (*b*) K. Pierloot, in *Computational Organometallic Chemistry*, ed. T. R. Cundari, Marcel Dekker, Basel, 2001, p. 123; (*c*) G. Franking and N. Fröhlich, *Chem. Rev.*, 2000, **100**, 717.
10 R. J. Bartlett, *Annu. Rev. Phys. Chem.*, 1981, **32**, 359.
11 W. A. Goddard, T. H. Dunning, W. J. Hunt and P. J. Hay, *Acc. Chem. Res.*, 1973, **6**, 368.
12 B. O. Ross, *Adv. Chem. Phys.*, 1987, **69**, 399.
13 K. Andersson, P. Å. Malmqvist and B. O. Ross, *J. Chem. Phys.*, 1992, **96**, 1218.
14 W. Kohn and L. J. Sham, *Phys. Rev. A*, 1965, **140**, 1133.
15 (*a*) W. Koch and M. C. Holthausen, *A Chemist's Guide to Density Functional Theory*, Wiley-VCH, Weinheim, 2000; (*b*) W. Kohn, A. D. Becke and R. G. Parr, *J. Phys. Chem.*, 1996, **100**, 12974; (*c*) R. G. Parr and W. Yang, *Density Functional Theory of the Electronic Structure of Molecules*, Oxford University Press, New York, 1989; (*d*) T. Ziegler, *Chem. Rev.*, 1991, **91**, 651; (*e*) *Chemical Applications of Density Functional Theory*, ed. B. B. Laird, R. Ross and T. Ziegler, American Chemical Society, Washington, 1996, 1997.
16 P. Hohenberg and W. Kohn, *Phys. Rev. B*, 1964, **136**, 864.
17 (*a*) A. D. Becke, *J. Chem. Phys*, 1986, **84**, 4524; (*b*) A. D. Becke, *J. Comput. Chem.*, 1999, **20**, 63; (*c*) A. D. Becke, *Phys. Rev. A*, 1988, **38**, 3098.
18 (*a*) J. P. Perdew, *Phys. Rev. B*, 1986, **33**, 8822; (*b*) J. P. Perdew, K. Burke and M. Ernzerhof, *Phys. Rev. Lett.*, 1996, **77**, 3865.
19 (*a*) C. Lee, W. Yang and R. G. Parr, *Phys. Rev. B*, 1988, **37**, 785; (*b*) Y. Zhang and W. Yang, *Phys. Rev. Lett.*, 1998, **80**, 890; (*c*) B. Hammer, L. B. Hansen and J. K. Nørskov, *Phys. Rev.*, 1999, **59**, 7413.
20 (*a*) A. D. Becke and M. R. Roussel, *Phys. Rev. A*, 1989, **39**, 3761; (*b*) V. Tschinke and T. Ziegler, *Can. J. Chem.*, 1989, **67**, 460; (*c*) E. Proynov, A. Vela and D. R. Salahub, *Chem. Phys. Lett.*, 1994, **230**, 419; (*d*) T. van Voorhis and G. E. Scuseria, *Mol. Phys.*, 1997, **92**, 601; (*e*) M. Filitov and W. Thiel, *Phys. Rev. A*, 1988, **57**, 189; (*f*) J. P. Perdew and A. Zunger, *Phys. Rev. B*, 1981, **23**, 5048; (*g*) S. Patchkovskii, J. Autschbach and T. Ziegler, *J. Chem. Phys.*, 2001, **115**, 26; (*h*) S. Patchkovskii and T. Ziegler, work in progress.
21 A. D. Becke, *J. Chem. Phys.*, 1993, **98**, 1372.
22 P. Pulay, *Mol. Phys.*, 1969, **17**, 197.
23 (*a*) A. Matveev, M. Staufer, M. Mayer and N. Rösch, *Int. J. Quantum Chem.*, 1999, **75**, 863; (*b*) M. R. Bray, R. T. J. Deeth, V. J. Paget and P. D. Sheen, *Int. J. Quantum Chem.*, 1997, **61**, 85; (*c*) O. Gonzalez, V. Branchadell, K. Monyeyne and T. Ziegler, *Inorg. Chem.*, 1998, **37**, 1744; (*d*) J. M. Fischer, W. E. Piers, T. Ziegler, L. R. MacGillivray and M. J. Zaworotko, *Chem. Eur. J.*, 1996, **2**, 120; (*e*) M. A. Pietsch, M. Couty and M. B. Hall, *J. Phys. Chem.*, 1995, **99**, 16315; (*f*) J. L. C. Thomas and M. B. Hall, *Organometallics*, 1997, **16**, 2318; (*g*) S. Niu and M. B. Hall, *J. Phys. Chem. A*, 1977, **101**, 1360; (*h*) M. A. Büjse and E. J. Baerends, *J. Chem. Phys.*, 1989, **93**, 4129.
24 T. Ziegler, in *Computational Thermochemistry*, ed. K. K. Irikura and D. J. Frurip, ACS Symposium Series 677, American Chemical Society, Washington, DC, p. 369.
25 M. R. A. Blomberg and P. E. M. Siegbahn, in *Computational Thermochemistry*, ed. K. K. Irikura and D. J. Frurip, ACS Symposium Series 677, American Chemical Society, Washington, DC, p. 197.
26 (*a*) P. Pyykkö, *Chem. Rev.*, 1988, **88**, 563; (*b*) B. A. Hess, in *Encyclopedia of Computational Chemistry*, ed. P. v. R. Schleyer, John Wiley & Sons, Chichester, 1998, p. 2499; (*c*) N. Kaltsoyannis, *J. Chem. Soc., Dalton Trans.*, 1997, 1.
27 (*a*) T. Ziegler, J. G. Snijders and E. J. Baerends, in *The Challenge of d and f Electrons*, ed. D. R. Salahub and M. Zerner, ACS Symposium Series 394, American Chemical Society, Washington, DC, p. 322; (*b*) L. Jian, G. Schreckenbach and T. Ziegler, *J. Am. Chem. Soc.*, 1995, **117**, 486; (*c*) T. Ziegler, *Can. J. Chem.*, 1995, **73**, 743.
28 J. Li and T. Ziegler, *Inorg. Chem.*, 1995, **34**, 3245.
29 (*a*) T. Ziegler, J. G. Snijders and E. J. Baerends, *J. Chem. Phys.*, 1981, **74**, 1271; (*b*) J. Autschbach and W. H. E. Schwarz, *Theor. Chem. Acc.*, 2000, **104**, 82.
30 (*a*) S. S. Nash and B. E. Bursten, *J. Phys. Chem. A*, 1999, **103**, 632; (*b*) E. M. Wezenbeek, E. J. Baerends and T. Ziegler, *Inorg. Chem.*, 1995, **34**, 238.
31 D. Heidrich, in *The Reaction Path in Chemistry*, ed. D. Heidrich, Kluwer Academic Publishers, Dordrecht, 1995, p. 1.
32 (*a*) I. V. Ionova and E. A. Carter, *J. Chem. Phys.*, 1994, **10**, 6562; (*b*) A. Ulitsky and R. J. Elber, *J. Chem. Phys.*, 1990, **92**, 1510; (*c*) E. Sandre, M. C. Payne, I. Stich and J. D. Gale, in *Transition State Modeling for Catalysis*, ed. D. G. Truhlar and K. Morokuma, ACS Symposium Series 721, American Chemical Society, Washington, DC, p. 346; (*d*) A. Banerjee, N. Adams, J. Simons and R. Shepard, *J. Phys. Chem.*, 1985, **89**, 52; (*e*) J. Baker, *J. Comput. Chem.*, 1986, **7**, 385.
33 K. Fukui, *Acc. Chem. Res.*, 1981, **14**, 363.
34 L. K. Johnson, S. Mecking and M. Brookhart, *J. Am. Chem. Soc.*, 1996, **118**, 267.
35 W. Yang and T.-S. Lee, *J. Chem. Phys.*, 1995, **103**, 5674.
36 (*a*) A. Warshel and M. Levitt, *J. Mol. Biol.*, 1976, **103**, 227; (*b*) U. C. Singh and P. A. Kollman, *J. Comput. Chem.*, 1986, **7**, 718; (*c*) M. Field, P. A. Bash and M. Karplus, *J. Comput. Chem.*, 1990, **11**, 700; (*d*) F. Maseras and K. Morokuma, *J. Comput. Chem*, 1995, **16**, 1170; (*e*) T. K. Woo, L. Cavello and T. Ziegler, *Theor. Chem. Acc.*, 1998, **100**, 307.
37 (*a*) F. Maseras, in *Computational Organometallic Chemistry*, ed. T. R. Cundari, Marcel Dekker, Basel, 2001, p. 159; (*b*) L. Deng, T. K. Woo, P. M. Margl and T. Ziegler, *J. Am. Chem. Soc.*, 1997, **119**, 6177; (*c*) M. Svensson, S. Humbel, R. D. J. Froese, T. Matsubara, S. Sieber and K. Morokuma, *J. Phys. Chem.*, 1996, **100**, 19357; (*d*) D. Bakowies and W. Thiel, *J. Phys. Chem.*, 1996, **100**, 10580; (*e*) P. Comba and T. W. Hambley, *Molecular Modeling of Inorganic Compounds*, Wiley-VCH, second edition, 2001.
38 O. Tapia and J. Bertrán, *Solvent Effects and Chemical Reactivity*, Kluwer, Dordrecht, 1996.
39 A. Klamt and G. Schuurmann, *J. Chem. Soc., Perkin Trans. 2*, 1993, 799.
40 (*a*) C. J. Cramer and D. G. Truhlar, in *Reviews in Computational Chemistry*, ed. K. B. Lipkowitz and D. B. Boyd, VCH Publishers, New York, 1995, vol. 6; (*b*) C. Pye and T. Ziegler, *Theor. Chem. Acc.*, 1999, **101**, 396.
41 J. Tomasi, *Chem. Rev.*, 1994, **94**, 2027.
42 Surface dipoles and other more complicated schemes can be envisioned.
43 J. Gao, in *Reviews in Computational Chemistry*, ed. K. B. Lipkowitz and D. B. Boyd, VCH, New York, 1996, vol. 7.
44 R. Car and M. Parrinello, *Phys. Rev. Lett.*, 1985, **55**, 2471.
45 A. Curioni, M. Sprik, W. Andreoni, H. Schiffer, J. Hutter and M. Parrinello, *J. Am. Chem. Soc.*, 1997, **119**, 7218.
46 M. E. Tuckerman, K. Laasonen, M. Sprik and M. Parrinello, *J. Phys. Chem.*, 1995, **99**, 5749.
47 J. Gao, *J. Acc. Chem. Res.*, 1992, **29**, 298.
48 T. K. Woo, P. E. Blöchl and T. Ziegler, *J. Mol. Struct.: THEOCHEM.*, 2000, **506**, 313.
49 *Inorganic Electronic Structure and Spectroscopy*, vol. I–II, ed. E. I. Solomon and A. B. P. Lever, Wiley, New York, 1999.
50 S. J. A. van Gisbergen, J. A. Groeneveld, A. Rosa, J. G. Snijders and E. J. Baerends, *J. Phys. Chem. A*, 1999, **103**, 6835.
51 H. Nakai, Y. Ohmori and H. Nakatsuji, *J. Chem. Phys.*, 1991, **95**, 8287.
52 T. Ziegler, A. Rauk and E. J. Baerends, *Theor. Chim. Acta*, 1977, **43**, 261; C. Daul, *Int. J. Quantum Chem.*, 1994, **52**, 867.
53 J. C. Slater, *Adv. Quantum Chem.*, 1972, **6**, 1.
54 (*a*) M. Petersilka, U. J. Grossmann and E. K. U. Gross, *Phys. Rev. Lett.*, 1996, **76**, 12; (*b*) C. Jamorski, M. E. Casida and D. R. Salahub, *J. Chem. Phys.*, 1996, **104**, 5134; (*c*) S. J. A. van Gisbergen, J. G. Snijders and E. J. Baerends, *J. Chem. Phys.*, 1995, **103**, 9347; (*d*) E. Runge and E. K. U. Gross, *Phys. Rev.*, 1980, **21**, A1561; (*e*) C. van Caillie and R. D. Amos, *Chem. Phys. Lett.*, 1998, **291**, 71.
55 (*a*) T. Ziegler, A. Rauk and E. J. Baerends, *J. Chem. Phys.*, 1976, **16**, 209; (*b*) A. Stückl, C. A. Daul and H. U. Güdel, *J. Chem. Phys.*, 1997, **107**, 4606; (*c*) B. O. Ross, *Acc. Chem. Res.*, 1999, **32**, 137.
56 S. J. A. van Gisbergen, C. Fonseca Guerra and E. J. Baerends, *J. Comput. Chem.*, 2000, **21**, 1511.
57 J. C. Corchado and D. G. Truhlar, in *Combined Quantum Mechanical and Molecular Mechanical Methods*, ed. J. Gao and

M. A. Thompson, ACS Symposium Series 712, American Chemical Society, Washington, DC, p. 106.
58 R. Car and M. Parrinello, *Phys. Rev. Lett.*, 1985, **55**, 2471.
59 (*a*) O. M. Aagaard, R. J. Meier and F. Buda, *J. Am. Chem. Soc.*, 1998, **120**, 7174; (*b*) H. M. Senn, P. E. Blöchl and A. Togni, *J. Am. Chem. Soc.*, 2000, 122; (*c*) F. De Angelis, A. Sgamellotti and N. Re, *Organometallics*, 2000, **19**, 4104.
60 (*a*) T. K. Woo, P. E. Blöchl and T. Ziegler, *J. Phys. Chem. A*, 2000, **104**, 121; (*b*) M. Cheong, R. Schmid and T. Ziegler, *Organometallics*, 2000, **19**, 1973.
61 (*a*) E. Pijper, G. J. Kroes, R. A. Olsen and E. J. Baerends, *J. Chem. Phys.*, 2000, **113**, 8300; (*b*) A. Jarid, M. Moreno, A. Lledos, J. M. Lluch and J. Bertran, *J. Am. Chem. Soc.*, 1993, **115**, 5861; (*c*) M.-C. Heitz and C. Daniel, *J. Am. Chem. Soc.*, 1997, **119**, 8269; (*d*) D. Guillaumont and C. Daniel, *J. Am. Chem. Soc.*, 1999, **121**, 11733; (*e*) F. Maseras, A. Lledós, E. Clot and Q. Eisenstein, *Chem. Rev.*, 2000, **100**, 601.
62 (*a*) W. J. Hehre, L. Radom, P. v. R. Schleyer and J. A. Pople, *Ab Initio Molecular Orbital Theory*, Wiley, New York, 1986; (*b*) B. C. Garrett and D. G. Truhlar, *J. Chem. Phys.*, 1979, **70**, 1593.
63 J. Baker, M. Muir and J. Andzelm, *J. Chem. Phys.*, 1995, **102**, 2063.
64 (*a*) C. W. Bauschlicher and P. Maitre, *Chem. Phys. Lett.*, 1996, **246**, 40; (*b*) P. E. M. Siegbahn, *Adv. Chem. Phys.*, 1996, XCIII; (*c*) J. F. Harrison, *Chem. Rev.*, 2000, **100**, 679.
65 (*a*) F. P. Rotzinger, *J. Am. Chem. Soc.*, 1997, **119**, 5230; (*b*) D. De Vito, H. Sidorenkova, F. P. Rotzinger, J. Weber and A. E. Merbach, *Inorg. Chem.*, 2000, **39**, 5547.
66 (*a*) R. J. Deeth and L. I. Elding, *Inorg. Chem.*, 1996, **35**, 5019; (*b*) Z. Lin and M. B. Hall, *Inorg. Chem.*, 1991, **30**, 646.
67 Y. Han, L. Deng and T. Ziegler, *J. Am. Chem. Soc.*, 1997, **119**, 5939.
68 (*a*) W. Wang and E. Weitz, *J. Phys. Chem.*, 1997, **101**, 2358; (*b*) D. Musaev and K. Morokuma, *J. Am. Chem. Soc.*, 1995, **117**, 799.
69 (*a*) S. Niu and M. B. Hall, *Chem. Rev.*, 2000, **100**, 353; (*b*) A. Dedieu, *Chem. Rev.*, 2000, **100**, 543.
70 (*a*) P. Margl, L. Deng and T. Ziegler, *J. Am. Chem. Soc.*, 1998, **120**, 5517; (*b*) K. Krogh-Jespersen and A. S. Goldman, in *Transition State Modeling for Catalysis*, ed. D. G. Truhlar and K. Morokuma, ACS Symposium Series 721, American Chemical Society, Washington, DC, p. 151; (*c*) Y.-D. Wu and Z.-H. Peng, in *Transition State Modeling for Catalysis*, ed. D. G. Truhlar and K. Morokuma, ACS Symposium Series 721, American Chemical Society, Washington, DC, p. 151; (*d*) E. Folga, T. K. Woo and T. Ziegler, in *Theoretical Aspects of Homogeneous Catalysis*, ed. P. W. N. M. van Leeuwen, Kluwer Academic Publishers, Dordrecht, 1995, p. 115; (*e*) F. Maseras, A. Lledós, E. Clot and E. Eisenstein, *Chem. Rev.*, 2000, **100**, 601.
71 (*a*) M. Mavrikakis, L. B. Hansen, J. J. Mortensen, B. Hammer and J. K. Nørskov, in *Transition State Modeling for Catalysis*, ed. D. G. Truhlar and K. Morokuma, ACS Symposium Series 721, American Chemical Society, Washington, DC, p. 245; (*b*) M. Neurock and V. Pallassana, in *Transition State Modeling for Catalysis*, ed. D. G. Truhlar and K. Morokuma, ACS Symposium Series 721, American Chemical Society, Washington, DC, p. 226; (*c*) J. L. Witten and H. Yang, in *Transition State Modeling for Catalysis*, ed. D. G. Truhlar and K. Morokuma, ACS Symposium Series 721, American Chemical Society, Washington, DC, p. 274.
72 (*a*) M. Torrent, M. Sola and G. Frenking, *Chem. Rev.*, 2000, **100**, 439; (*b*) S. A. Blaszkowski and R. A. van Santen, in *Transition State Modeling for Catalysis*, ed. D. G. Truhlar and K. Morokuma, ACS Symposium Series 721, American Chemical Society, Washington, DC, p. 307; (*c*) J. Sauer, M. Sierka and F. Haase, in *Transition State Modeling for Catalysis*, ed. D. G. Truhlar and K. Morokuma, ACS Symposium Series 721, American Chemical Society, Washington, DC, p. 358; (*d*) R. A. Friesner and B. D. Dunietz, *Acc. Chem. Res.*, 2001, **34**, 351; (*e*) P. E. M. Siegbahn and M. R. A. Blomberg, *Chem. Rev.*, 2000, **100**, 421; (*f*) G. H. Loew and D. L. Harris, *Chem. Rev.*, 2000, **100**, 42.
73 D. L. Beveridge and F. M. DiCapua, *Annu. Rev. Biophys. Chem.*, 1989, **18**, 431.
74 (*a*) E. A. Carter, G. Ciccotti, J. T. Hynes and R. Kapral, *Chem. Phys. Lett.*, 1989, **156**, 472; (*b*) E. Paci, G. Ciccotti, M. Ferrario and R. Kapral, *Chem. Phys. Lett.*, 1991, **176**, 581.
75 (*a*) P. Margl, T. Ziegler and P. Blöchl, *J. Am. Chem. Soc.*, 1995, **117**, 12625; (*b*) P. Margl, T. Ziegler and P. E Blochl, *J. Am. Chem. Soc.*, 1996, **118**, 5412; (*c*) P. Margl, J. C. W. Lohrenz, T. Ziegler and P. Blochl, *J. Am. Chem. Soc.*, 1996, **118**, 4434; (*d*) T. K. Woo, P. M. Margl, P. E. Blöchl and T. Ziegler, *J. Am. Chem. Soc.*, 1996, **118**, 13021; (*e*) T. K. Woo, P. Margl and T. Ziegler, *Organometallics*, 1997, **16**, 3454–3468; (*f*) P. M. Margl, T. K. Woo, P. E. Blöchl and T. Ziegler, *J. Am. Chem. Soc.*, 1998, **120**, 217; (*g*) T. K. Woo, P. E. Blöchl and T. Ziegler, *J. Phys. Chem. A*, 2000, **104**, 121; (*h*) T. K. Woo, P. M. Margl, L. Deng and T. Ziegler, *ACS Symposium Series 712*, ed. J. Gao and M. A. Thompson, American Chemical Society, Washington, DC, 1998; pp. 128–148; (*i*) T. K. Woo, P. M. Margl, L. Deng, L. Cavallo and T. Ziegler, *ACS Symposium Series 721*, ed. D. G. Truhlar and K. Morokuma, American Chemical Society, Washington, DC, 1999, pp. 173–187; (*j*) T. K. Woo, P. M. Margl, L. Deng, L. Cavallo and T. Ziegler, *Catal. Today*, 1999, **50**, 479.
76 (*a*) B. Ensing, E. J. Meijer, P. E. Blöchl and E. J. Baerends, *J. Phys. Chem. A*, 2001, **105**, 3300; (*b*) T. K. Woo, P. E. Blöchl and T. Ziegler, *J. Mol. Struct.: THEOCHEM.*, 2000, **506**, 313.
77 F. Hirata, H. Sato, S. Ten-no and S. Kato, in *Combined Quantum Mechanical and Molecular Mechanical Methods*, ed. J. Gao and M. A. Thompson, ACS Symposium Series 712, American Chemical Society, Washington, DC, p. 188.
78 (*a*) J. C. Tully, *Faraday Discuss.*, 1998, **110**, 407; (*b*) M. Garavelli, F. Bernardi, M. Olivucci, T. Vreven, P. Celani and M. A. Robb, *Faraday Discuss.*, 1998, **110**, 51; (*c*) D. G. Truhlar, *Faraday Discuss.*, 1998, **110**, 521.